ELSEVIER

Earth and Planetary Science Letters 140 (1996) 97–112

EPSL

Evolution of Pangea: paleomagnetic constraints from the Southern Alps, Italy

Giovanni Muttoni [a,1], Dennis V. Kent [a,*], James E.T. Channell [b]

[a] *Lamont-Doherty Earth Observatory, Columbia University, Palisades, NY 10964, USA*
[b] *Department of Geology, University of Florida, Gainesville, FL 32611, USA*

Received 3 October 1995; accepted 6 February 1996

Abstract

A new early Late Triassic paleopole for Adria has been obtained from the Val Sabbia Sandstone in the Southern Alps. As Early Permian and Jurassic–Cretaceous paleomagnetic data from para-autochthonous regions of Adria such as the Southern Alps are consistent with 'African' APWPs [1,2], paleomagnetic data from this region can be used to bolster the West Gondwana APWP in the poorly known Late Permian–Triassic time interval. The Southern Alpine paleopoles are integrated with the West Gondwana and Laurussia APWPs of Van der Voo [1] and used to generate a tectonic model for the evolution of Pangea. The Early Permian overall mean paleopole for West Gondwana and Adria, in conjunction with the coeval Laurussia paleopole, support Pangea B of Morel and Irving [3]. The Late Permian/Early Triassic and the Middle/Late Triassic paleopoles from Adria and Laurussia support Pangea A-2 of Van der Voo and French [4]. The phase of transcurrent motion between Laurasia and Gondwana [5] that caused the Pangea B to A-2 transition occurred essentially in the Permian (at the end of Variscan orogeny) with an average relative velocity of approximately 10 cm/yr. Finally, the Late Triassic/Early Jurassic paleopoles from West Gondwana and Laurussia agree with Pangea A-1 of Bullard et al. [6], the widely accepted Pangea configuration at the time of the Jurassic breakup.

Keywords: Pangaea; paleomagnetism; Val Sabbia Sandstone; Triassic; apparent polar wandering; Lombardy Italy

1. Introduction

A variety of models for the reconstruction of Pangea have been proposed since the original 'Wegener' fit, but the position of Gondwana versus Laurasia in a Pangea supercontinental assembly remains controversial. West Gondwana (i.e., Africa and South America) and Laurussia (North America, Greenland and Europe) provide the main body of paleomagnetic data for Gondwana and Laurasia, respectively. There are numerous Early Permian to Early Jurassic paleopoles from North America and Europe which delineate a well-defined apparent polar wander path (APWP) [1,7]. However, between the Early Permian and the Late Triassic/Early Jurassic, the APWP for West Gondwana is generally poorly defined, and there are inconsistencies of unclear origin in the sparse paleomagnetic data from East Gondwana (India, Australia, Antarctica and Madagascar) [1].

* Corresponding author. E-mail: dvk@ldeo.columbia.edu
[1] Present address: Istituto per la Geologia Marina, Consiglio Nazionale delle Ricerche, via Gobetti, 101-40129 Bologna, Italy.

PII S0012-821X(96)00038-6

The African affinity of Permian and Mesozoic paleomagnetic directions from Adria (the peri-Adriatic fold-belt and related foreland) has been documented in previous reviews [1,2,8,9]. Interpretations have been controversial due to ubiquitous, many counterclockwise, thrust sheet rotations in the Apennines and poor knowledge of the African APWP. According to a recent analysis, available Permian to Cretaceous paleopoles from the Southern Alps and other para-autochthonous regions of Adria (Istria, Apulia and Iblei) agree internally, and are consistent with 'African' polar wander paths [2].

The Adria APWP is not well defined in the Middle to Late Triassic interval (see [10]). We therefore undertook a paleomagnetic study of Carnian (lower Upper Triassic) red beds of the Lombardy region of the central Southern Alps. We then generated a set of mean Southern Alpine paleopoles for Early Permian to Triassic time and used them as proxies for the West Gondwana APWP in intervals for which reliable African/South American data are scarce. The composite West Gondwana APWP and the Laurussia APWP of Van der Voo [1] are then used to test alternative Pangea fits [3,4,6], and gener-

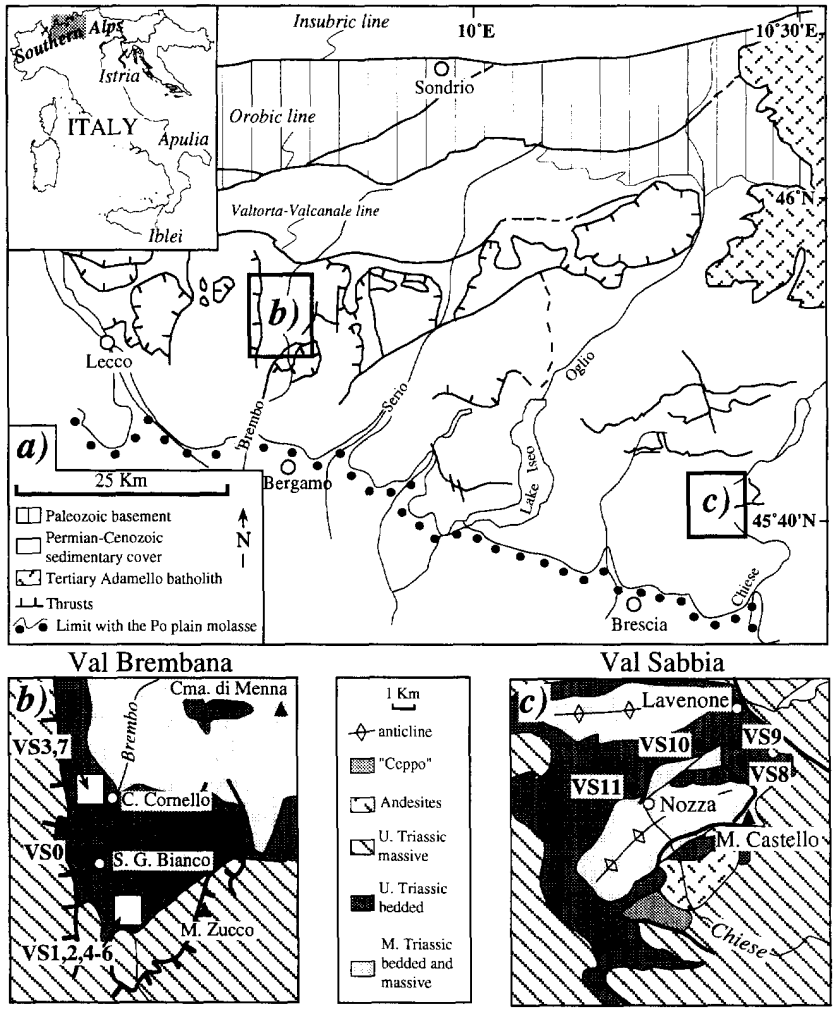

Fig. 1. (a) Sketch map of the Lombardian Alps. (b) and (c) Geologic maps of the Val Brembana and Val Sabbia areas, respectively, with the location of the sampling sites.

ate a model for the evolution of Pangea in the Early Permian to Early Jurassic.

2. Carnian red beds from the Southern Alps

2.1. Geology

The Southern Alps are a south-vergent fold and thrust belt resulting from Africa–Europe convergence during the Late Cretaceous–Cenozoic (see [11] and references therein). The Southern Alps are bounded to the north by the Insubric Line, and are partly buried under the Po Plain molasse to the south. The structural model for the Southern Alps, inferred from a variety of geophysical, structural and geological data, is also constrained by paleomagnetic directions, which indicate that the south-vergent tectonic transport did not involve appreciable differential rotation among thrusted units [12], at least for those regions investigated by paleomagnetism.

The Carnian sedimentary sequence of Lombardy (central Southern Alps) shows the transition from Lower Carnian shallow-water carbonates (Breno Formation and Calcare Metallifero Bergamasco) to a fluviodeltaic–lagoonal–carbonate platform system (represented by the Val Sabbia Sandstone, the Gorno Fm. and the Breno Fm., respectively) during the early–middle Carnian [13]. During the Late Carnian the siliciclastic San Giovanni Bianco Fm. prograded over much of the Val Sabbia–Gorno–Breno triplet [13]. We focused our attention on the Val Sabbia Sandstone in Val Brembana (Fig. 1a,b) and Val Sabbia (Fig. 1a, c). The Val Sabbia Sandstone con-

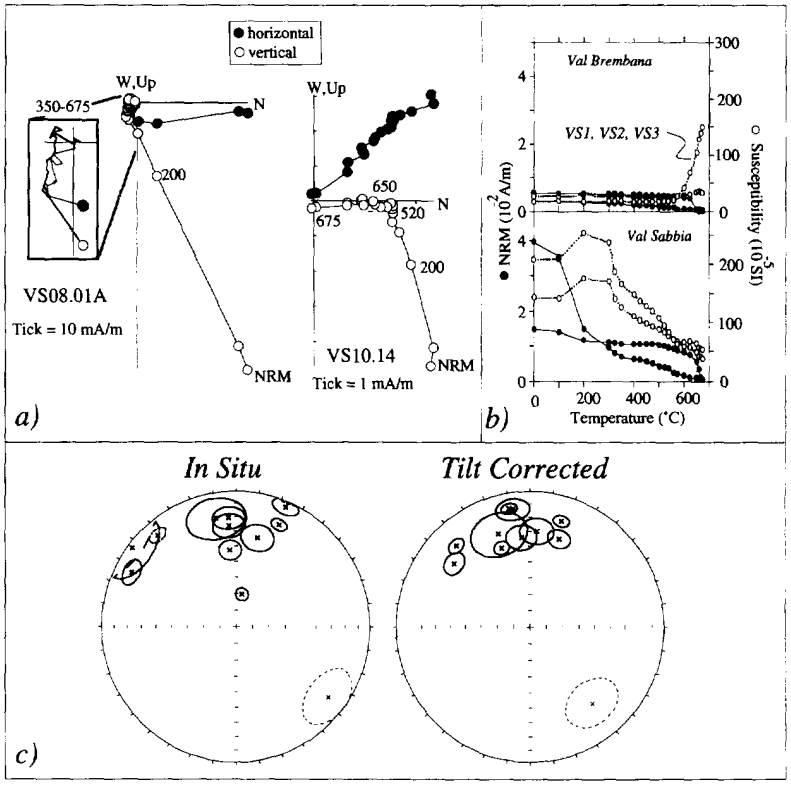

Fig. 2. (a) Vector end-point demagnetization diagrams of representative samples from the Val Sabbia Sandstone. Open symbols = projections onto the vertical plane; solid symbols = projections onto the horizontal plane. All diagrams are in situ coordinates. (b) Thermal variations of Natural Remanent Magnetization and initial (volume) susceptibility for representative Val Sabbia Sandstone samples from Val Brembana and Val Sabbia. (c) Site-mean directions of the characteristic component from the Val Sabbia Sandstone projected on the lower hemisphere of equal-area projection.

sists of greenish-grey to red, fine to medium-grained siltstones and sandstones of volcanic origin [13]. No age-diagnostic fossils have yet been found in the Val Sabbia Sandstone [13]; its inferred early–middle Carnian age is based on stratigraphic relationships with surrounding fossiliferous formations. The Gorno Fm., which interfingers with the Val Sabbia Sandstone, is paleontologically attributed to the early–middle Carnian [14]. The main body of the Gorno Fm. ('main Gorno' of Garzanti [13]), interfingering with the upper Val Sabbia Sandstone, contains a Middle Carnian pelecypod fauna, whilst the overlying San Giovanni Bianco Fm. contains Late Carnian *Neomegalodon* [14]. Thus, the Val Sabbia Sandstone is constrained to an early/middle Carnian age.

In central Val Brembana, to the south of the Valtorta–Valcanale fault system (Fig. 1a), the Middle/Upper Triassic sedimentary sequence is relatively undisturbed, with a southerly regional vergence of low-angle thrusts (Fig. 1b). At the site scale, bedding strike is westerly to southwesterly and usually moderately inclined to shallow. In Val Sabbia, the Triassic sequence is arranged in a series of east–west to northeast–southwest trending folds (Fig. 1c). In this region, dips vary from steep northerly to moderate towards the east and south.

Table 1
Characteristic magnetization directions from the Val Sabbia Sandstone

		In Situ				Tilt Corrected			
Site	n/n'	D(°)	I(°)	k	a95(°)	D(°)	I(°)	k	a95(°)
VS0	6/6	355.2	42.7	104	6.6	340.1	37.9	249	4.3
VS1	10/9	356.0	20.6	40	8.2	351.6	13.5	40	8.2
VS2	10/7	14.0	32.8	46	9.0	4.3	29.8	46	9.0
VS3	14/9	349.5	19.7	13	15.1	341.3	28.3	13	15.1
VS5	16/16	357.6	28.0	36	6.2	356.5	35.9	36	6.3
VS6	18/18	23.1	19.4	72	4.1	16.7	19.5	72	4.1
VS7	19/19	22.9	4.6	30	6.2	18.7	31.9	30	6.2
VS8	14/14	127.4	-15.4	8	15.1	140.9	-28.1	8	15.1
VS9	16/16	297.2	13.5	34	6.4	309.6	27.3	34	6.4
VS10	17/17	319.2	-12.0	65	4.5	317.5	19.8	65	4.5
VS11	15/15	10.3	70.2	96	3.9	349.9	12.6	96	3.9
MEAN	11 sites	349.0	25.8	6.0	20.9	346.1	27.6	13.5	12.9

Paleomagnetic pole: Latitude = 57.0° N, Longitude = 215.3° E, dp/dm = 7.7°/14.1°

Sites VS0–VS7 from Val Brembana and VS8–VS11 from Val Sabbia localities. n/n' = number of samples thermally demagnetized/number of samples used for statistical analysis; D = declination; I = inclination; k = precision parameter; a95 = semi-angle of cone of 95% confidence about the mean direction; dp, dm = semi-axes of the confidence oval about the paleomagnetic pole.

2.2. Paleomagnetism

Samples for paleomagnetic analysis were collected from the Val Sabbia Sandstone at Val Brembana (Fig. 1a,b) and Val Sabbia (Fig. 1a,c) with a portable petrol-powered drill and were oriented using a magnetic compass. From each 2.5 cm diameter core sample, one or two standard 11cc specimens were cut. The total number of sites and specimens analysed is 12 and 175, respectively (3 and 34, respectively, of them are from [15]). All the specimens were subjected to complete stepwise thermal demagnetization. Remanence measurements were performed on a 2G 3-axis cryogenic magnetometer located in a magnetically shielded room at Lamont-Doherty. Mineral alterations after each heating step were monitored by measurements of low field susceptibility with a Bartington MS2 Meter. Least-squares line fitting [16] was used to determine the component directions in demagnetization intervals chosen by eye from orthogonal projections. Mean directions were calculated using standard Fisher statistics.

Orthogonal projections of thermal demagnetization data indicate the presence of two stable magnetization components (Fig. 2a). A low unblocking temperature component consistent with the present-day field direction was removed initially at some sites (VS0, VS2, VS9 and VS10). A dual polarity characteristic component, distributed in orientation from northwest and down (southeast and up) to north-northeast and down, was successively unblocked at all sites except VS4 (Fig. 2a). For Site VS4, demagnetization diagrams are inconsistent with the other sites and magnetization components are poorly defined. This site may have been affected by its proximity to a major south-vergent thrust plane and the data have been excluded from the Val Sabbia Sandstone overall mean direction.

The maximum unblocking temperature (680°C) of the natural remanent magnetization (NRM) is consistent with the presence of hematite as the main magnetic remanence carrier (Fig. 2b). The sites from Val Brembana (VS0–VS7) have lower NRM intensities (1–12 mA/m) and susceptibilities ($< 50 \times 10^{-5}$ SI)

Table 2
Permian to Triassic paleomagnetic poles from the Southern Alps with quality factor Q ≥ 3

	Rock Unit	Locality	Age	°N	°E	°A95 (dp/dm)	1	2	3	4	5	6	7	Q	Reference
VS	Val Sabbia Ss.	Lombardy	Early/Middle Carnian	57.0	215.3	(7.7/14.1)	x	x	x	x	x	x	x	7	this study
17	Ladinian-Carnian volcs.	Dolomites	Ladinian-Carnian	48.0	240.0	9	x	x		x	x		x	5	[35]
16	Buchenstein Formation	Dolomites	Anisian/Ladinian boundary	64.3	212.0	(4.0/6.8)	x	x	x			x		4	[Muttoni et al., unpub.]
15	Prezzo Limestone	Southern Alps	late Anisian	63.2	229.3	8	x	x	x	x	x			5	[10]
14	Valle di Scalve porph.	Lombardy	Middle Triassic	52.0	221.0	6	x		x		x		x	4	[33]
	MEAN (N=5)	*Southern Alps*	*Middle/early Late Triassic*	*57.3*	*224.5*	*9 [K = 74]*									
13	Werfen Formation	Dolomites	Scythian (Early Triassic)	42.0	233.0	(3.4/6.8)	x	x	x	x	x	x	x	7	[39]
12	Verrucano Lombardo Ss.	Lombardy	Late Permian	43.0	241.0	(3.9/7.5)	x	x	x		x		x	5	[15]
11	Staro & Camparmo volcs.	Vicentinian Alps	Late Permian	53.0	241.0	6	x		x		x	x	x	5	[37]
10	Val Gardena Ss.	Dolomites	Late Permian	51.0	235.0		x		x		x		x	4	[38]
9	Verrucano Lombardo Ss.	Lombardy	Late Permian	48.0	239.0	5	x	x	x		x		x	5	[36]
8	Val Gardena Ss.	Vicentinian Alps	Late Permian	48.0	238.0	7	x				x		x	3	[37]
7	Verrucano Lomb. metased.	Lombardy	Late Permian	47.0	237.0	6	x		x		x	x	x	5	[36]
6	Val Gardena Ss.	Dolomites	Late Permian	42.0	237.0	18	x			x	x		x	4	[35]
	MEAN (N=8)	*Southern Alps*	*L. Permian/E. Triassic*	*46.8*	*237.6*	*3.1 [K = 317]*									
5	Bolzano quartz porph. comb.	Dolomites	Early Permian	45.0	239.0	4	x	x	x	x	x		x	6	[34]
4	Lugano (Ganna) porphyries	Ticino	Early Permian	43.0	243.0	10	x	x	x	x	x		x	6	[18]
3	Lower Collio & Auccia volc.	Lombardy	Early Permian	39.0	252.0	20	x		x		x		x	4	[33]
2	Arona volcanics	Lombardy	Early Permian	35.0	248.0	14	x	x	x		x		x	5	[18]
1	Auccia volcanics	Lombardy	Early Permian	38.0	245.0	8	x	x	x		x		x	5	[18]
	MEAN (N=5)	*Southern Alps*	*Early Permian*	*40.1*	*245.6*	*5.2 [K = 220]*									

°N, °E = latitude and longitude of paleomagnetic pole; K = precision parameter; A95 = radius of cone of 95% confidence about the pole; (dp/dm = semi-axes of oval of 95% confidence about the pole). Reliability criteria and Q factor for poles 1–14 and 17 from [1], where 1 = well-determined rock age; 2 = sufficient number of samples; 3 = adequate demagnetization; 4 = field tests; 5 = structural control; 6 = presence of reversals; 7 = no resemblance to paleopoles of younger age.

than sites from Val Sabbia (VS8–VS11), where values are in the 5–58 mA/m and 100–200 $\times 10^{-5}$SI ranges, respectively. Sites from Val Brembana (VS1, VS2 and VS3) occasionally show a large increase in susceptibility above 600°C, due to mineral alteration during the heating procedure. In these cases, the characteristic component was poorly defined and data from these samples was rejected (10% of samples rejected at site VS1, 30% at site VS2 and 36% at site VS3).

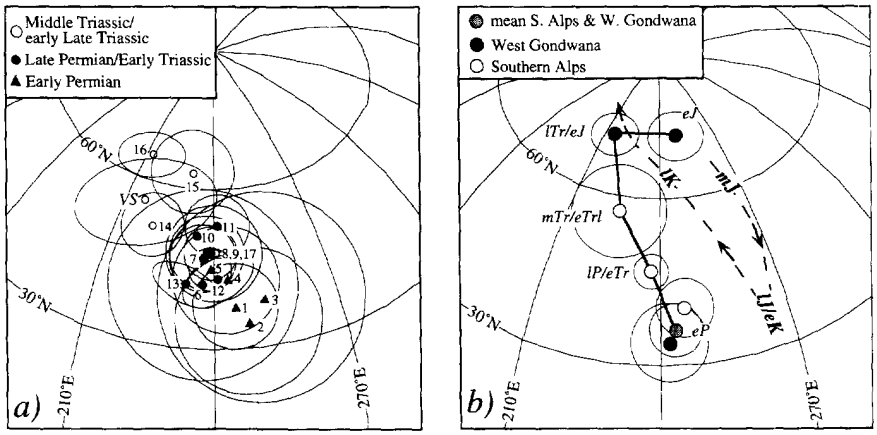

Fig. 3. (a) Early Permian to Middle/early Late Triassic paleomagnetic poles from the Southern Alps with Van der Voo [1] quality factor Q ≥ 3 (Table 2). (b) Early Permian to Early Jurassic master apparent polar wander path for West Gondwana (solid line and dots). The track of the Jurassic and Cretaceous polar wander path for Adria and 'Africa' (dashed line), inferred from Channell [2], is shown for reference. eP = Early Permian; lP/eTr = Late Permian/Early Triassic; mTr/eTrl = Middle Triassic/early Late Triassic; lTr/eJ = Late Triassic/Early Jurassic; eJ = Early Jurassic.

The in situ characteristic directions are distributed in distinct groups by site (Fig. 2c, Table 1). After correction for bedding tilt, the characteristic component site-mean directions (from all the sites except VS4) converge, and the precision parameter (k) increases during progressive tilt correction such that the ratio of k after to before tilt correction reaches a maximum (2.25) at 100% tilt correction, providing a fold test positive at the 95% confidence level [17] (Fig. 2c). The resolved magnetization components therefore pre-date the Late Cretaceous/Early Cenozoic folding and may represent the Carnian geomagnetic field. It should be noted that the tilt-corrected site-mean declinations are more scattered than the inclinations (Fig. 2c), indicating between-site true or apparent rotations, which we assume are randomly distributed. The overall mean direction is $Dec = 346.1°E$, $Inc = 27.6°$ ($a95 = 12.9°$, $k = 13.5$, $N = 11$) (Table 1), although the error estimate is only approximate because of the oval distribution of directions. The corresponding mean pole is located at 57°N, 215.3°E, yielding a paleolatitude of 14.6°N for a nominal site location at 45.5°N, 10°E.

2.3. Comparison to Southern Alps data

Early Permian to Triassic paleomagnetic poles from the Southern Alps with quality factor $Q \geq 3$ [1], including the Val Sabbia pole (Table 2), show an age-progressive trend over about 30° of latitude (Fig. 3a). The five Early Permian and eight Late Permian/Early Triassic poles yield well-defined mean poles (Table 2, [33–39], Fig. 3b). Van der Voo [1] reports the Early Permian poles of Table 2 as latest Carboniferous/Early Permian. The volcanic cycle in the central Southern Alps, however, is generally referred to as the Early Permian [18–20].

Middle/early Late Triassic poles from the Southern Alps are somewhat more scattered (Fig. 3a) and yield a mean pole with a cone of confidence (9°) that is larger than preceding or succeeding time intervals (Table 2, Fig. 3b). Nevertheless, this mean pole is representative of a wide variety of lithologies, as it is based on volcanic, volcaniclastic, tuffaceous and deep-water carbonate rocks from Lombardy and the Dolomites. Among them is the pole (#15) obtained from the Middle Triassic Prezzo Limestone [10]. The high latitude of the Prezzo Limestone pole is confirmed by the Val Sabbia pole, as well as by a pole (#16) based on 92 samples from the Anisian/Ladinian (Middle Triassic) Frötschbach section from the Dolomites [Muttoni et al., unpubl.] that gave a pattern of magnetic reversals which correlates with the pattern of the coeval Aghia Triada section from Hydra (Greece) [21]. The Mesozoic

Table 3
Early Permian to Early Jurassic mean paleomagnetic poles for West Gondwana and Laurussia apparent polar wander paths

West Gondwana and Southern Alps							Laurussia						Laurussia rotated [a]		
Age	°N	°E	K	A95	N	Reference	Age	°N	°E	K	A95	N	Reference	°N	°E	Δ
eJ	72.0	248.5	108	4.7	10 (WG)	[1] [b]	eJ	68.0	91.0	156	3.2	14	[1] [e]	69.6	247.6	2.4
lTr/eJ	71.1	214.8	458	4.3	4 (WG)	[1] [c]	lTr/eJ	61.0	81.0	68	4.7	15	[1] [e]	69.4	224.0	3.5
mTr/eTrl	57.3	224.5	74	9.0	5 (SAlps)	this study	lTrm/lTr	51.0	96.0	64	5.5	12	[1] [e]	56.5	222.4	1.4
lP/eTr	46.8	237.6	317	3.1	8 (SAlps)	this study	lP/eTr	51.2	114.2	118	2.2	35	[1] [e,f]	49.9	238.0	3.1
eP	36.2	243.3	77	4.8	13 (5 SAlps, 8 WG) [d]	this study	eP	46.0	124.0	161	1.9	35	[1] [e]	42.0	241.9	5.9

Abbreviations as in Table 2 with N = number of entries; WG = West Gondwana; SAlps = Southern Alps; eP = Early Permian; lP/eTr = Late Permian/Early Triassic; mTr/eTrl = Middle Triassic/early Late Triassic; lTrm/lTr = late Middle Triassic/Late Triassic; lTr/eJ = Late Triassic/Early Jurassic; eJ = Early Jurassic. The mean West Gondwana (Laurussia) paleopoles are calculated by averaging paleopoles from Africa, South America and the Southern Alps (North America and Europe) in the coordinate system of northwest Africa (North America) according to the rotation parameters of Lottes and Rowley [22] (Bullard et al. [6]). Southern Alps paleopoles are from Table 2. [a] Laurussia paleopoles rotated about a Euler pole at 75.4°N, 352.9°E, $\Omega = 98.4°$ counterclockwise (this study); Δ = the angular distance between the West Gondwana and the rotated Laurussia paleopoles. [b] From table 5.8. [c] Late Triassic/Early Jurassic mean paleopole for West Gondwana of table 5.8 in [1] does not correspond to the mean of the four entries on which it is based, and thus was recalculated. [d] WG poles are from table A4 in [1] and constitute the Early Permian mean pole of table 5.8 in [1] at 34°N, 242°E (K = 60, A95 = 7°). [e] From table 5.7. [f] Late Permian/Early Triassic Laurussia mean pole combines the 11 Late Permian and the 24 Early Triassic individual poles for Laurussia from tables A1–A3 in [1] which constitute the Late Permian and Early Triassic mean poles of table 5.7 in [1].

loop of the 'African' and Southern Alpine APWPs [2] brings the Late Cretaceous and Late Triassic poles close to one another (Fig. 3b), so that the age of remanence acquisition cannot be determined simply on the basis of the pole position.

3. Comparison of West Gondwana and Southern Alps data

The Early Permian to Middle/early Late Triassic polar wander path for the Southern Alps is compared with selected mean paleomagnetic poles for the Early Permian and Late Triassic/Early Jurassic of West Gondwana [1], transferred into northwest Africa coordinates using rotation parameters of Lottes and Rowley [22] (Fig. 3b). Eight Early Permian poles from South America and Africa give a mean pole (Table 3) that is statistically indistinguishable from the coeval pole from the Southern Alps at the 99% confidence level [23] (Fig. 3b). No reliable ($Q \geq 3$) Late Permian–Middle Triassic poles are available for West Gondwana [1] whereas the Late Triassic/Early

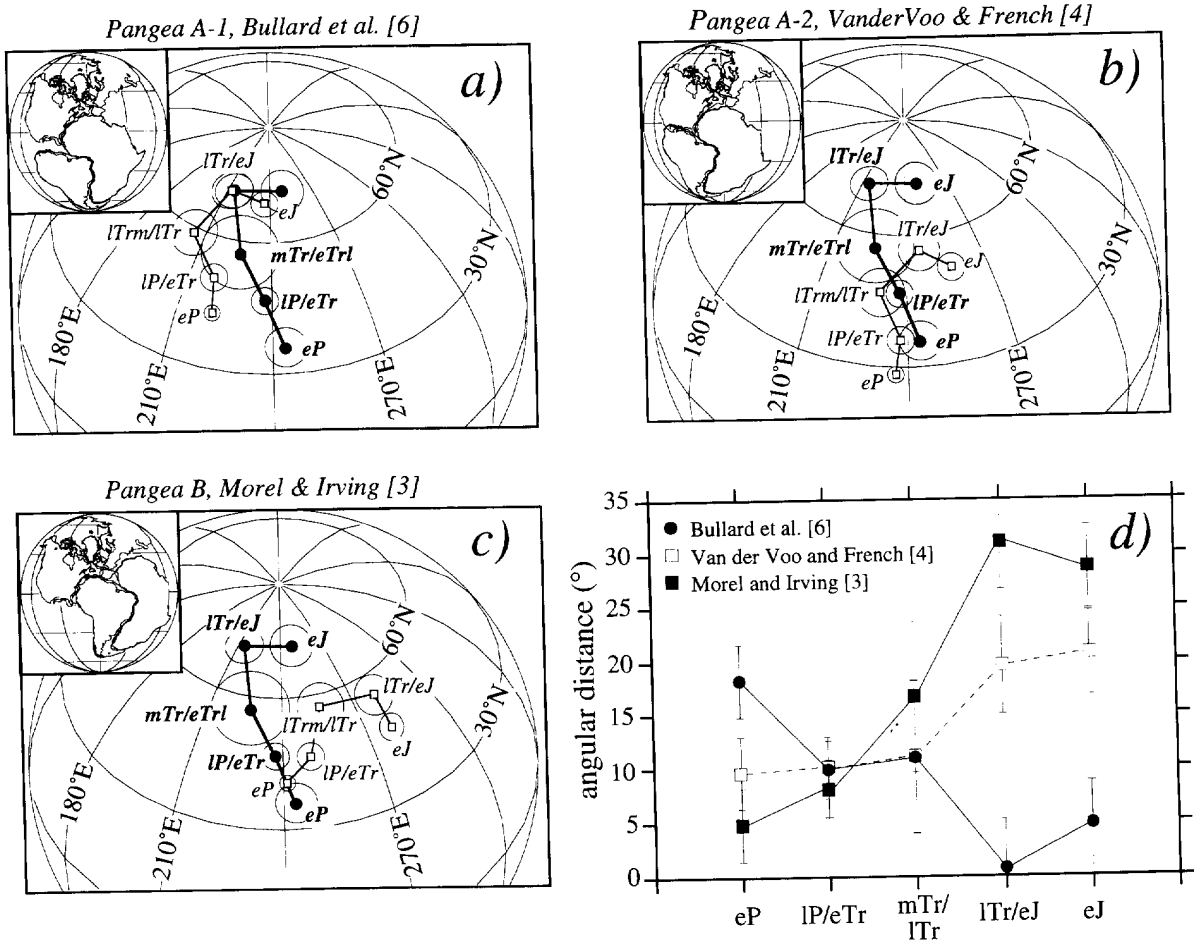

Fig. 4. The master West Gondwana APWP (dots) and the Laurussia APWP of Van der Voo [1] (open squares) tested against alternative Pangea fits. The West Gondwana APWP is in northwest Africa coordinates. Laurussia poles are rotated to (northwest) Africa coordinates according to: (a) Bullard et al. [6], Euler pole at 67.7°N, 346°E, angle of rotation (Ω) 74.8° counterclockwise (ccw); (b) Van der Voo and French [4], Euler pole at 57°N, 339.2°E, $\Omega = 88.9°$ ccw; (c) Morel and Irving [3], Euler pole at 34°N, 359°E, $\Omega = 77°$ ccw. (d) Plot of the angular distance between rotated Laurussia and West Gondwana poles. eP = Early Permian; lP/eTr = Late Permian/Early Triassic; mTr/eTrl = Middle Triassic/early Late Triassic (West Gondwana); lTrm/lTr = late Middle Triassic/Late Triassic (Laurussia); mTr/lTr = Middle Triassic/Late Triassic (in d); lTr/eJ = Late Triassic/Early Jurassic; eJ = Early Jurassic.

Jurassic and the Early Jurassic mean paleomagnetic poles are based on four and ten entries, respectively (Table 3). The Early Permian and Late Triassic/Early Jurassic mean poles for West Gondwana overlap and bracket the Early Permian to Middle/early Late Triassic mean poles for the Southern Alps. These data suggest that the close concordance of the Southern Alps/Africa APWPs for the Jurassic–Cretaceous [2] extends back to at least Early Permian times. We conclude that the para-autochthonous Southern Alps moved in concert with Africa during most of the Late Paleozoic and Mesozoic. Data from para-autochthonous Southern Alps can thus be used to construct a better defined APWP for West Gondwana.

A master APWP for the Early Permian to Early Jurassic of West Gondwana has been constructed by adopting: (1) the overall mean Early Permian pole obtained by combining data from the Southern Alps and West Gondwana; (2) the Late Permian/Early Triassic and Middle/early Late Triassic mean poles from the Southern Alps; and, finally, (3) the Late Triassic/Early Jurassic and Early Jurassic mean poles from West Gondwana (Fig. 3b; Table 3). The dashed line in Fig. 3b marks the combined autochthonous Adria–'Africa' APWP of Channell [2] for Jurassic and Cretaceous times.

4. Comparison of West Gondwana and Laurussia APWPs in a test of different Pangea reconstructions

There seems to be a consensus that the Atlantic Ocean opened in the Jurassic from a Pangea A-type configuration as obtained by placing Northwest Africa and South America adjacent to eastern North America and southern North America, respectively (e.g., [4,6]). There is considerable disagreement, however, regarding the geometry of Pangea during earlier times. For example, Irving [24] and Morel and Irving [3] placed Africa adjacent to Europe, and South America adjacent to eastern North America during the Early Permian (Pangea B), whereas Smith et al. [25] carried this even further, and placed South America and Africa to the south of Europe and Asia, respectively (Pangea C).

The composite West Gondwana APWP of this study and the Laurussia APWP of Van der Voo [1] are compared in a test of different Pangea reconstructions. The six time intervals used to construct the Early Permian–Early Jurassic APWP for Laurussia have been reduced to five time intervals for a more direct comparison with the West Gondwana APWP (Table 3). This was done by merging the 11 Late Permian and the 24 Early Triassic entries of Van der Voo [1] into an average pole representative of Late Permian/Early Triassic time. We also regard the late Middle Triassic/Late Triassic pole for Laurussia [1] as being approximately coeval to the Middle Triassic/early Late Triassic pole for West Gondwana (i.e., as Middle/Late Triassic). The Laurussia APWP in North American coordinates has been transferred to African coordinates using three different rotation parameters, those of Bullard et al. [6], Van der Voo and French [4] and Morel and Irving [3] (Fig. 4).

Bullard et al. [6] closed the Atlantic Ocean by minimizing the gaps and overlaps between the Atlantic continental margins at the 500 fathom isobath. The Pangea configuration that they obtained is referred to as Pangea A-1 by Morel and Irving [3], and it is the one that leaves the modern Gulf of Mexico open (see the inset in Fig. 4a). When the Laurussia APWP is transferred to African coordinates according to Bullard et al. [6], the two paths agree only at the younger end (Late Triassic/Early Jurassic and Early Jurassic) and are increasingly divergent with older age, differing by about 18° (±5.2°) in the Early Permian (Fig. 4a,d). This conclusion confirms the observation of other investigators (e.g., [3,4]), that the Pangea A-1 configuration does not satisfy the paleopoles for this entire time interval.

In an attempt to reconcile the well-known discrepancy in the APWPs, Van der Voo and French [4] proposed a modification of the Bullard fit in which West Gondwana is rotated 20° clockwise so that the northwestern edge of South America is tightly adjacent to the North American Gulf Coast region and the modern Gulf of Mexico is, consequently, closed. This configuration has been named Pangea A-2 by Morel and Irving [3] (see inset in Fig. 4b). When the Laurussia APWP is rotated into African coordinates according to Van der Voo and French [4], Laurussia and West Gondwana APWPs lie along similar meridians but are offset in age along their track, especially in the Late Triassic/Early Jurassic (19.5° ± 6.4°)

and Early Jurassic (21° ± 5.7°) intervals (Fig. 4b, d). A certain agreement is reached only in the middle (Triassic) part of the APWPs.

Pangea B of Irving [24] and Morel and Irving [3] places northwestern South America adjacent to eastern North America (see inset in Fig. 4c); it provides a good match only for Early Permian poles for Laurussia and West Gondwana, with an increasing divergence for the younger poles; for example, 31° (±6.4°) in the Late Triassic/Early Jurassic (Fig. 4c, d).

This analysis confirms the long-standing conclusion that none of the above Pangea reconstructions optimize the *entire* Laurussia and West Gondwana APWPs for the Early Permian to the Early Jurassic. Instead, each of the Pangea reconstructions seems to match coeval paleomagnetic poles for different intervals of time: Pangea A-1 for the Late Triassic/Early Jurassic, Pangea B for the Early Permian and Pangea A-2 as a Triassic compromise.

5. Evolution of Pangea

The Early Permian–Jurassic portion of the Laurussia and West Gondwana APWPs are very similar

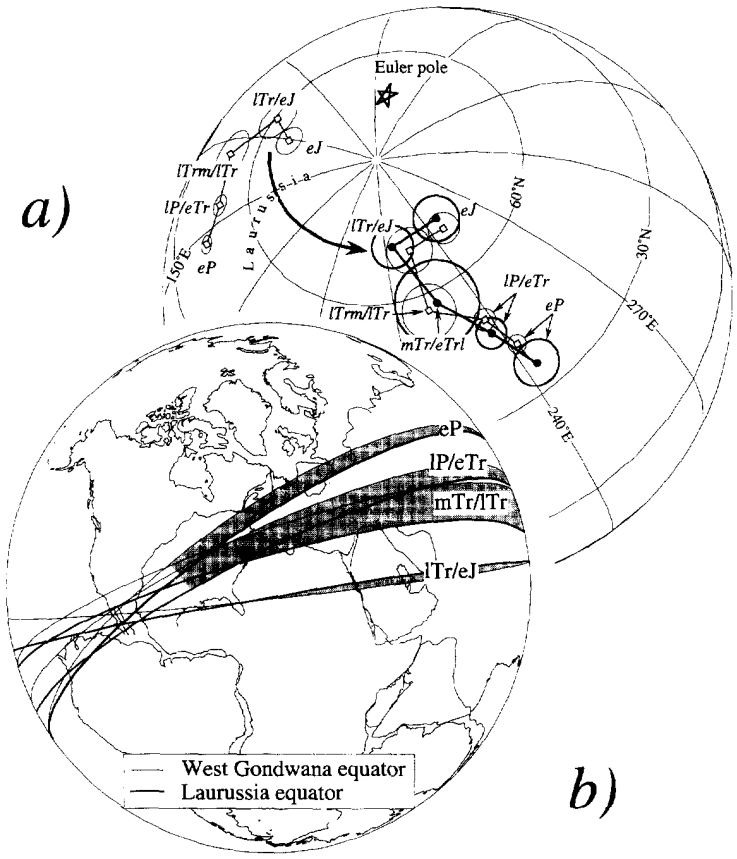

Fig. 5. (a) The master West Gondwana APWP (dots) in northwest Africa coordinates compared to the Laurussia APWP of Van der Voo [1] (open squares) which is also shown rotated with respect to a pole at 75.4°N, 352.9°E ($\Omega = 98.4°$ ccw) for a best fit to West Gondwana APWP. (b) Pangea reconstruction obtained by rotating Laurussia about a pole at 75.4°N, 352.9°E, $\Omega = 98.4°$ ccw, which makes APWPs closely coincide. The paleo-equators of Laurussia and West Gondwana for the Early Permian to Late Triassic/Early Jurassic are also shown. Early Jurassic paleo-equators, which are not reported, are most similar to the Late Triassic/Early Jurassic paleo-equators. Age abbreviations *are* as in Fig. 4.

in shape. This qualitative observation is confirmed by the correspondence of these APWPs after a simple rotation of the Laurussia APWP about an approximate best-fit Euler pole located at 75.4°N, 352.9°E (angle of rotation 98.4°) (Fig. 5a). Rotated Laurussia paleopoles lie within just a few degrees of coeval West Gondwana poles (median angular difference of 3.1°) and are statistically indistinguishable at the 99% confidence level [23] from Late Permian to the Early Jurassic time. Only the Early Permian poles do not agree precisely, but they are offset by only 5.9° (±5.2°) along track. The similarity in shapes of these APWPs suggests that the main elements of Pangea (i.e., Laurussia and West Gondwana) were closely associated.

If Pangea is reconstructed by strictly using this Euler pole, a large overlap between North America and West Gondwana results (Fig. 5b). There is no paleomagnetic constraint on longitude, however, so that Gondwana can be displaced relative to Laurasia along lines of latitude without affecting the correspondence in APWPs. The paleo-equators for Laurasia and Gondwana for the Early Permian–Early Jurassic give the reference frame for this longitudinal shift, and also indicate that Pangea rotates systematically over the entire period of time (Fig. 5b), suggesting a continuous evolution which we explore in a series of reconstructions that satisfy the paleomagnetic constraints and use geologic criteria to optimize the longitudinal indeterminacy.

Pangea is portrayed in four different time intervals (namely, Early Permian, Late Permian/Early Triassic, Middle/Late Triassic and Late Triassic/Early Jurassic), corresponding to the four mean paleopoles for Laurussia and West Gondwana (Table 3). (Pangea in the Early Jurassic is not shown as it is virtually the same as Pangea in the Late Triassic/Early Jurassic.) The reconstructions have been made by the following process: (1) elements of Gondwana have been rotated relative to northwest Africa according to the parameters of Lottes and Rowley [22], and oriented with respect to lines of paleolatitude using West Gondwana mean paleopoles; (2) elements of Laurasia have been rotated relative to North America with the parameters of Bullard et al. [6], and oriented with lines of paleolatitude using Laurussia mean poles; and (3) the position of Laurasia has been adjusted longitudinally to eliminate the overlaps with Gondwana. The longitudinal shift adopted is usually the one that keeps Pangea as tightly closed as possible. The Euler poles for the four reconstructions are listed in Table 4.

Table 4
Euler Poles for the Pangea reconstructions

		Early Permian			Late Permian/ Early Triassic			Middle/ Late Triassic			Late Triassic/ Early Jurassic		
		°N	°E	Ω(°)	°N	°E	Ω(°)	°N	°E	Ω(°)	°N	°E	Ω(°)
1	NWAF	01.75	149.84	50.87	01.25	144.44	41.48	00.00	314.50	-35.70	00.00	304.80	-18.90
2	NEAF->NWAF	00.66	153.04	56.34	-00.07	148.70	46.77	-01.21	140.58	40.77	-03.25	136.39	23.37
3	SAF->NWAF	02.39	154.76	57.27	01.86	150.97	47.53	00.91	143.39	41.20	-00.35	141.76	23.66
4	SAM->NWAF	58.62	109.39	45.74	65.71	085.92	42.14	63.76	058.05	40.83	62.17	002.44	43.06
5	AR->NWAF	-00.55	160.09	61.09	-01.96	157.16	51.26	-03.54	150.72	44.60	-09.03	152.59	27.37
6	MAD->NWAF	04.06	166.98	43.19	01.79	165.40	33.05	-02.29	157.56	25.74	-17.15	179.12	09.63
7	ANT->NWAF	-45.58	-109.45	10.12	-42.78	-046.58	14.82	-39.53	-023.40	21.41	-22.47	-026.17	36.88
8	IND->NWAF	-01.40	-164.44	97.06	-04.98	-163.63	88.24	-07.77	-164.79	80.71	-16.90	-156.98	70.87
9	NA	30.02	47.50	51.27	58.03	056.20	72.75	59.18	039.00	74.19	64.60	024.00	71.42
10	EU->NA	-13.42	67.02	44.39	35.07	075.60	43.94	37.47	057.92	44.56	43.99	042.40	39.40
11	GRN->NA	12.75	60.61	49.80	48.18	071.25	62.44	51.05	055.71	62.89	57.95	043.72	58.26

°N and °E = latitude and longitude of the Euler pole; Ω (°) = the angle of rotation about the Euler pole (counterclockwise when positive). Continents are denoted as follows: NWAF = northwest Africa and Adria; NEAF = northeast Africa; SAF = South Africa; SAM = South America; AR = Arabia; MAD = Madagascar; ANT = Antarctica; IND = India; NA = North America; EU = Eurasia; GRN = Greenland. (1) positioned with respect to mean paleomagnetic pole (within a95 error); (2)–(8) calculated by matrix multiplication of poles from Lottes and Rowley [22] and pole (1); (9) calculated by matrix multiplication of mean paleomagnetic pole (within a95 error) and a pole centered at 90°N with an arbitrary rotation to eliminate overlap between Laurussia and West Gondwana; (10) and (11) calculated by matrix multiplication of poles from Bullard et al. [6] and pole (9).

5.1. Early Permian

The reconstruction of Pangea that satisfies the Early Permian paleopoles is remarkably similar to Pangea B of Irving [24] and Morel and Irving [3] (Fig. 6). As discussed by them, Pangea B provides a symmetrical framework for the Appalachian–Hercynian (Varisican) fold belt, placing the Appalachians of eastern North America opposite to the northwestern South America fold belt, and the Hercynian fold belt of Europe opposite to the northwestern Africa fold belt of the Mauritanides. Pangea B also provides space for the Gulf of Mexico units (chiefly, the Yucatán–Campeche unit) that collided with the southern margin of North America during the Middle Carboniferous–Middle Permian to form the Marathon–Ouichita fold-belt [26].

To the east, Tethys is much narrower between Asia and Africa than in a Pangea A-type configuration. Florida is tentatively placed to the south of Europe, along the northwestern Africa coast, in the gap between South America and Africa. The available Ordovician–Silurian paleomagnetic data support the idea that Florida was part of West Gondwana at least in the Paleozoic [27]. Protruding from the northern Africa margin is the Adria promontory. The

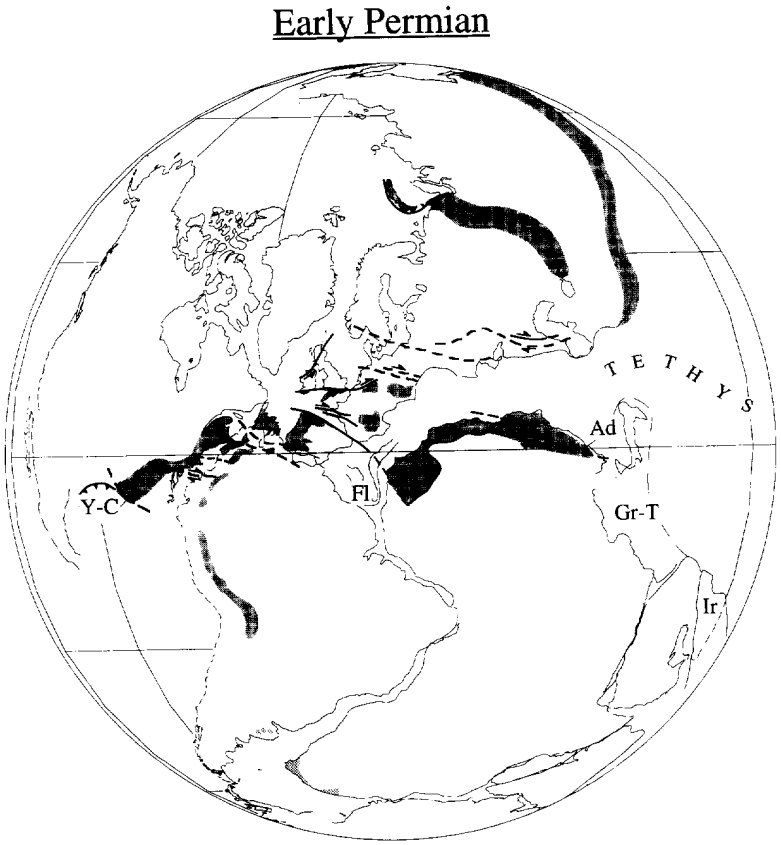

Fig. 6. Pangea model that satisfies the Early Permian mean paleopoles from Laurussia and West Gondwana (within the α_{95} cones of confidence); this configuration resembles Pangea B of Morel and Irving [3]. *Y–C* = the Yucatán–Campeche unit; *Fl* = Florida; *Ad* = Adria; *Gr–T* = an unsubdivided Greco–Turkish unit; *Ir* = the Iran–Afghanistan–Mega Lhasa unit(s) of [40]. The distribution of the Hercyinides (grey pattern) is from Morel and Irving [3]. Tectonic lines are from Arthaud and Matte [5].

attachment of the promontory to Africa is an explicit assumption in the construction of the West Gondwana APWP.

5.2. Late Permian / Early Triassic

The reconstruction of Pangea that satisfies the Late Permian/Early Triassic paleopoles is similar to Pangea A-2 of Van der Voo and French [4] (Fig. 7). A dextral megashear between Laurasia and Gondwana has apparently brought northwest Africa adjacent to eastern North America.

Arthaud and Matte [5] documented an important Late Varisican deformation event which affected the southern Appalachians, the Mauritanides and the Urals. This event was associated with Late Carboniferous dextral shear and Permian transtensional tectonics, caused by the relative motion of Laurasia to the north and Gondwana to the south. We propose that this Permo–Carboniferous shear/transtension is associated with the evolution from Pangea B to Pangea A-2 by the Late Permian/Early Triassic, that is, toward the end of the Varisican tectonic episode.

5.3. Middle / Late Triassic

The Middle/Late Triassic reconstruction of Pangea (Fig. 8) is less reliable compared to the previous ones, because the Middle/early Late Triassic West Gondwana mean paleopole for this time is poorly defined relative to the other mean paleopoles (Table 3). The general configuration is, however,

Fig. 7. Pangea model that satisfies the Late Permian/Early Triassic mean paleopoles from Laurussia and West Gondwana (within the α_{95} cones of confidence); this configuration resembles Pangea A-2 of Van der Voo and French [4].

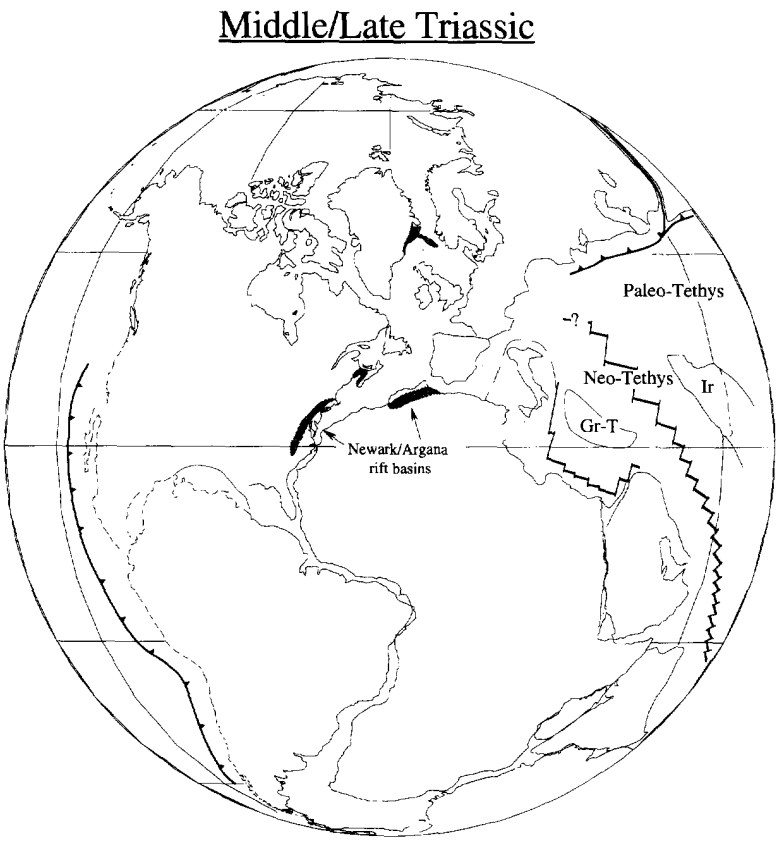

Fig. 8. Pangea model that satisfies the Middle/Late Triassic mean paleopoles from Laurussia and West Gondwana (within the α_{95} cones of confidence); this configuration resembles Pangea A-2 of Van der Voo and French [4].

virtually the same as for the Late Permian/Early Triassic; that is, essentially Pangea A-2, with Pangea shifted to the north by a few degrees.

5.4. Late Triassic / Early Jurassic

During the Late Triassic/Early Jurassic, Gondwana and Laurasia reached a configuration very close to that of Pangea A-1 of Bullard et al. [6] (Fig. 9). The Gulf of Mexico is opened as Gondwana rotated approximately 20° counterclockwise with respect to Laurasia about a Saharan Euler pole.

Predominantly distensional tectonics took place, starting in the Early Jurassic, in the Gulf of Mexico region between the Yucatán–Florida Straits unit(s) and the Guyana shield [26], as well as between eastern North America and northwest Africa–Iberia. This rifting was preceded by the formation of rift-related basins of the Newark–Argana type during the Late Triassic, stretching from Newfoundland–Iberia–Agadir, in the north, to southeastern U.S.–Senegal in the south, often filled with thousands of meters of continental, lacustrine, evaporitic and marginal-marine sediments. The rifting of Pangea had commenced, with the subsequent formation of the Atlantic Ocean as discussed elsewhere (e.g., [32]).

6. Discussion

Selected ($Q \geq 3$) paleomagnetic data from the literature and the present study from the Southern Alps are used to refine the West Gondwana APWP for the Early Permian to Late Triassic/Early Jurassic, an interval of time for which data from Africa

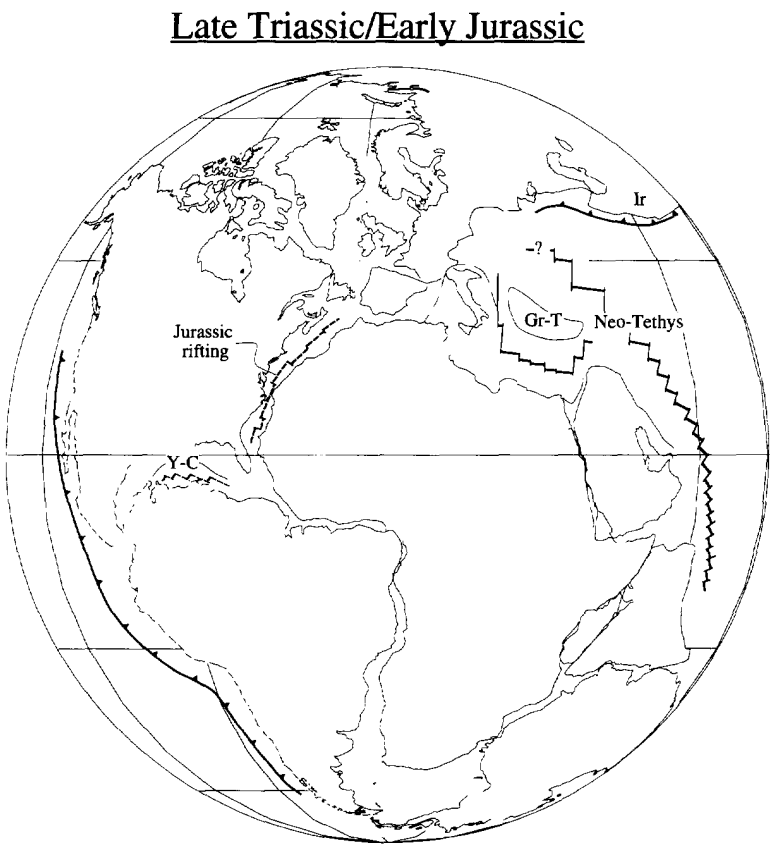

Fig. 9. Pangea model that satisfies Late Triassic/Early Jurassic mean paleopoles from Laurussia and West Gondwana; this configuration resembles Pangea A-1 of Bullard et al. [6].

and South America are sparse. Comparison of the refined West Gondwana APWP with the Laurussia APWP of Van der Voo [1] shows that the two paths are very similar in shape, indicating that West Gondwana and Laurussia were closely associated over this interval in a Pangea configuration. However, any single standard Pangea model (A-1, A-2 or B) does not account for the APWPs over the entire interval of time from the Early Permian to Late Triassic/Early Jurassic. Instead, an evolution of Pangea is indicated. The longitude indeterminacy of the paleomagnetic data, in conjunction with geological constraints, allow us to outline a tectonic evolution of Pangea that optimizes the matching of APWPs.

The Pangea B model of Irving [24] and Morel and Irving [3] is supported by Early Permian paleomagnetic data from West Gondwana and Laurussia. We note that this is the case with or without the inclusion of Southern Alps poles. The Pangea C model of Smith et al. [25] is not required, since the APWP constraints allow sufficient space for South America to be fitted in the gap between eastern North America and Iberia without introducing appreciable overlaps.

Southern Alpine proxy data for West Gondwana for the Late Permian/Early Triassic, in conjunction with coeval poles for Laurussia, are compatible with a reconstruction resembling Pangea A-2 of Van der Voo and French [4], therefore implying that the Pangea B to Pangea A-2 transition occurred between the Early Permian and the Late Permian/Early Triassic. Irving [24] and Morel and Irving [3] suggested that the transition from Pangea B to Pangea A, with

≈ 3500 km of relative motion, extended over the Triassic. The Permian transition proposed here would require a more rapid relative rate of motion (ca. 10 cm/yr), but would be confined within an interval of known dextral shear/transtension in the late stages of Varisican deformation, as documented by Arthaud and Matte [5]. The overall magnitude of relative motion is acknowledged as large but it may have been distributed over a broad zone, from the Donetz Basin to the southern Appalachians via Europe, and many of the wrench faults, sensu Arthaud and Matte [5], may lie undetected beneath more recent rocks. The Permian transition also obviates the need for purely transform faults, sought by Smith and Livermore [28] to account for the lack of Triassic deformation associated with a transition that was thought to occur at this time.

Southern Alpine and Laurussia data support Pangea A-2 also for the Middle/Late Triassic, but Late Triassic/Early Jurassic data from West Gondwana and Laurussia are more compatible with the Pangea A-1 of Bullard et al. [6], which is the generally accepted model of Pangea immediately prior to the Jurassic breakup [29]. The evolution from Pangea A-2 to Pangea A-1 was previously thought to have occurred from the Late Permian to the Middle Triassic ([30], see also [31]).

The internal mobility of Pangea implied by our analysis has implications for plate driving forces. The facing elements of Pangea, West Gondwana and Laurussia, experienced a differential counterclockwise rotation associated with a generalized dextral megashear/transtension from the Early Permian to Early Jurassic (Fig. 5b). Laurussia was translated by ≈ 3500 km dextrally with respect to West Gondwana essentially in the Permian, with an additional dextral motion occurring sometime prior to the Jurassic breakup. We note that Late Carboniferous data [1] allow a looser arrangement of Laurussia versus West Gondwana as the Pangea elements began to coalesce. The Permian shear is closely associated with the late stages of the Varisican collision and may predate the development of the Neo-Tethys spreading centers and Paleo-Tethys subduction in the Late Permian. The later Pangea A-2 to A-1 transition, however, may be related to the Neo-Tethys opening and Paleo-Tethys subduction.

Acknowledgements

This research was supported by the US National Science Foundation (grant ATM93-17227 to DVK) and the Doherty Senior Scientist endowment fund (post-doctoral fellowship to GM). We thank Jim Briden, Ted Irving, and Neil Opdyke for constructive reviews of the manuscript. Lamont-Doherty Earth Observatory contribution 5454. *[CL]*

References

[1] R. Van der Voo, Paleomagnetism of the Atlantic, Tethys and Iapetus Oceans, 411 pp., Cambridge University Press, Cambridge, 1993.

[2] J.E.T. Channell, Palaeomagnetism and palaeogeography of Adria, in: Palaeomagnetism and Tectonics of the Mediterranean Region, A. Morris and D.H. Tarling, eds., Geol. Soc. London Spec. Publ. 105, 119–132, 1996.

[3] P. Morel and E. Irving, Paleomagnetism and the evolution of Pangea, J. Geophys. Res. 86, 1858–1987, 1981.

[4] R. Van der Voo and R.B. French, Apparent polar wandering for the Atlantic-Bordering continents: Late Carboniferous to Eocene, Earth Sci. Rev. 10, 99–119, 1974.

[5] F. Arthaud and P. Matte, Late Paleozoic strike-slip faulting in southern Europe and northern Africa: Result of a right-lateral shear zone between the Appalachians and the Urals, Geol. Soc. Am. Bull. 88, 1305–1320, 1977.

[6] E.C. Bullard, J.E. Everett and A.G. Smith, A symposium on continental drift. IV. The fit of the continents around the Atlantic, Philos. Trans. R. Soc. London Ser. A 258, 41–51, 1965.

[7] R. Van der Voo, Phanerozoic paleomagnetic poles from Europe and North America and comparisons with continental reconstructions, Rev. Geophys. 28, 167–206, 1990.

[8] F. Heller, W. Lowrie and A.M. Hirt, A review of palaeomagnetic and magnetic anisotropy results, in: Alpine Tectonics, M.P. Coward, D. Dietrich and R.G. Park, eds., Geol. Soc. London Spec. Publ. 45, 399–420, 1989.

[9] J.E.T. Channell, B. D'Argenio and F. Horvath, Adria, the African promontory, in Mesozoic Mediterranean palaeogeography, Earth Sci. Rev. 15, 213–292, 1979.

[10] G. Muttoni and D.V. Kent, Paleomagnetism of late Anisian (Middle Triassic) sections of the Prezzo Limestone and the Buchenstein Formation, Southern Alps, Italy, Earth Planet. Sci. Lett. 122, 1–18, 1994.

[11] D. Roeder, South-Alpine thrusting and trans-Alpine convergence, in: Alpine Tectonics, M.P. Coward, D. Dietrich and R.G. Park, eds., Geol. Soc. London Spec. Publ. 45, 211–227, 1989.

[12] J.E.T. Channell, C. Doglioni and J.S. Stoner, Jurassic and Cretaceous paleomagnetic data from the Southern Alps (Italy), Tectonics 11(4), 811–822, 1992.

[13] E. Garzanti, Source rock versus sedimentary control on the mineralogy of deltaic volcanic arenites (Upper Triassic, Northern Italy), J. Sediment. Petrol. 56(2), 267–275, 1985.
[14] R. Assereto and P. Casati, Revisione della stratigrafia permo-triassica della Val Camonica meridionale (Lombardia), Riv. Ital. Paleontol. Stratigraf. 71(4), 999–1097, 1965.
[15] G. Muttoni, Preliminary results on the paleomagnetism of Upper Permian Verrucano Lombardo Sandstones from Val Camonica and of Upper Triassic Val Sabbia Sandstones from Val Brembana, Southern Alps, Natura Bresciana, Ann. Mus. Civ. Sci. Nat. Brescia 30, in press.
[16] J.L. Kirschvink, The least-squares line and plane and the analysis of palaeomagnetic data, Geophys. J. R. Astron. Soc. 62, 699–718, 1980.
[17] M.W. McElhinny, Statistical significance of the fold test in palaeomagnetism, Geophys. J. R. Astron. Soc. 8, 338–340, 1964.
[18] C. Heiniger, Paleomagnetic and rock magnetic properties of the Permian volcanics in the western Southern Alps, J. Geophys. 46, 397–411, 1979.
[19] A. Montrasio, Carta Geologica della Lombardia scala 1:250.000, Istituto Poligrafico e Zecca dello Stato, Roma, 1990.
[20] G. Cassinis, C. Neri and C.R. Perotti, The Permian and Permian–Triassic Boundary in Eastern Lombardy and Western Trentino (Southern Alps, Italy), in: The Nonmarine Triassic, S.G. Lucas and M. Morales, eds., N. M. Mus. Nat. Hist. Sci. Bull. 3, 51–63, 1993.
[21] G. Muttoni, J.E.T. Channell, A. Nicora and R. Rettori, Magnetostratigraphy and biostratigraphy of an Anisian–Ladinian (Middle Triassic) boundary section from Hydra (Greece), Palaeogeogr. Palaeoclimatol. Palaeoecol. 111, 249–262, 1994.
[22] A.L. Lottes and D.B. Rowley, Reconstruction of the Laurasian and Gondwanan segments of Permian Pangaea, in: Palaeozoic Palaeogeography and Biogeography, W.S. McKerrow and C.R. Scotese, eds., Geol. Soc. London Mem. 12, 383–395, 1990.
[23] P.L. McFadden and D.L. Jones, The fold test in palaeomagnetism, Geophys. J. R. Astron. Soc. 67, 53–58, 1981.
[24] E. Irving, Drift of the major continental blocks since the Devonian, Nature 270, 304–309, 1977.
[25] A.G. Smith, A.M. Hurley and J.C. Briden, Phanerozoic Paleocontinental World Maps, 102 pp., Cambridge University Press, Cambridge, 1981.
[26] J.L. Pindell, Alleghenian reconstruction and subsequent evolution of the Gulf of Mexico, Bahamas, and Proto-Caribbean, Tectonics 4, 1–39, 1985.
[27] N.D. Opdyke, D.S. Jones, B.J. MacFadden, D.L. Smith, P.A. Mueller and R.D. Shuster, Florida as an exotic terrane: paleomagnetic and geochronologic investigations of Lower Paleozoic rocks from the subsurface of Florida, Geology 15, 900–903, 1987.
[28] A.G. Smith and R.A. Livermore, Pangea in Permian to Jurassic time, Tectonophysics 187, 135–179, 1991.
[29] R.A. Livermore, A.G. Smith and F.J. Vine, Late Palaeozoic to early Mesozoic evolution of Pangea, Nature 322, 362–365, 1986.
[30] R. Van der Voo, F.J. Mauk and R.B. French, Permian–Triassic continental configurations and the origin of the Gulf of Mexico, Geology 4, 177–180, 1976.
[31] M.T. Swanson, Preliminary model for an early transform history in central Atlantic rifting, Geology 10, 321–324, 1982.
[32] K.D. Klitgord and H. Schouten, Plate kinematics of the central Atlantic, in: The Geology of North America, The Western North Atlantic Region, B.E. Tucholke and P.R. Vogt, eds., Vol. M, pp. 351–378, Geol. Soc. Am., Boulder, Colo., 1986.
[33] J.D.A. Zijderveld and K.A. De Jong, Paleomagnetism of some Late Paleozoic and Triassic rocks from the eastern Lombardic Alps, Geol. Mijnbouw. 48, 559–564, 1969.
[34] J.D.A. Zijderveld, G.J.A. Hazeu, M. Nardin and R. Van der Voo, Shear in the Tethys and the Permian paleomagnetism in the Southern Alps, including new results, Tectonophysics 10, 639–661, 1970.
[35] M. Manzoni, Paleomagnetic data of Middle and Upper Triassic age from the Dolomites (eastern Alps, Italy), Tectonophysics 10, 411–424, 1970.
[36] R. Kipfler and F. Heller, Palaeomagnetism of Permian red beds in the contact aureole of the tertiary Adamello intrusion (northern Italy), Phys. Earth Planet. Inter. 52, 365–375, 1988.
[37] J. De Boer, The Geology of the Vicentinian Alps with Special Reference to their Paleomagnetic History, 178 pp., Geologica Ultraiectina, 1963.
[38] R. Guicherit, Gravity Tectonics, Gravity Field, and Paleomagnetism in Northeast Italy, 125 pp., Geologica Ultraiectina, 1964.
[39] J.E.T. Channell and C. Doglioni, Early Triassic paleomagnetic data from the Dolomites (Italy), Tectonics 13(1), 157–166, 1994.
[40] J. Dercourt, L.E. Ricou and B. Vrielynck, Atlas Tethys Palaeoenvironmental Maps, 307 pp., Gauthier-Villars, Paris, 1993.